Polarization around an ion in a dielectric continuum with truncated electrostatic interactions

Nathan A. Baker[a] and Philippe H. Hünenberger
Department of Chemistry and Biochemistry, University of California, San Diego, La Jolla, California 92093-0365

J. Andrew McCammon
Department of Chemistry and Biochemistry, Department of Pharmacology, University of California, San Diego, La Jolla, California 92093-0365

(Received 26 January 1999; accepted 17 March 1999)

In order to reduce computational effort and to allow for the use of periodic boundary conditions, electrostatic interactions in explicit solvent simulations of molecular systems do not obey Coulomb's law. Instead, a number of ''effective potentials'' have been proposed, including truncated Coulomb, shifted, switched, reaction-field corrected, or Ewald potentials. The present study compares the performance of these schemes in the context of ionic solvation. To this purpose, a generalized form of the Born continuum model for ion solvation is developed, where ion–solvent and solvent–solvent interactions are determined by these effective potentials instead of Coulomb's law. An integral equation is formulated for calculating the polarization around a spherical ion from which the solvation free energy can be extracted. Comparison of the polarizations and free energies calculated for specific effective potentials and the exact Born result permits an assessment of the accuracy of these different schemes. Additionally, the present formalism can be used to develop corrections to the ionic solvation free energies calculated by molecular simulations implementing such effective potentials. Finally, an arbitrary effective potential is optimized to reproduce the Born polarization. © *1999 American Institute of Physics.* [S0021-9606(99)51822-9]

I. INTRODUCTION

The accurate representation of electrostatic interactions in molecular simulations of liquids and solutions has presented a difficult challenge to the scientific community.[1–5] This difficulty arises because

(i) approximations made in the treatment of electrostatic interactions are often among the most severe in a simulation procedure,
(ii) many simulated observables are extremely sensitive to these approximations,
(iii) and the calculation of electrostatic interactions is usually the most computationally expensive component of a simulation.

Explicit solvent simulations of bulk phase systems are usually performed under periodic boundary conditions. In this case, lattice-sum and related methods[4,6–8] appear as a natural choice to calculate electrostatic interactions. Although such methods are becoming increasingly popular, they are often difficult to implement and can be computationally demanding. Furthermore, the validity of approximating an inherently non-periodic system (solution) by an exactly periodic one (crystal) has been questioned.[9,10] In the best case, simulated properties may be corrected for the effect of artificial periodicity after the simulation.[7,9,11–13]

As an alternative to lattice-sum methods, one popular method involves the truncation of electrostatic interactions at a convenient cutoff distance, generally smaller than half the edge of the unit cell. However, cutoff truncation has been shown, using both explicit and implicit solvent models, to cause severe artifacts in simulations of liquids,[14–17] solvated ions,[18–22] ion pairs,[22–28] and biomolecules.[29–32] To remedy these artifacts, a number of modifications of the Coulomb potential below the cutoff distance have been proposed. In the case of switching and shifting functions,[33,34] the modification is purely empirical, causing the potential and its derivative to vanish at the cutoff distance. In the case of reaction-field corrections,[35–40] the modification of the Coulomb potential below the cutoff distance attempts to include the mean effect (reaction potential) arising from the presence of a dielectric continuum outside the cutoff sphere.

The simplest problem where the accurate treatment of electrostatic interactions is essential is the computation of ionic solvation free energies.[7,9,11–13,18–21] These free energies can, in principle, be calculated from continuum electrostatics by use of the Born model.[41] This model is based on three fundamental assumptions:

(a) The ion is a nonpolarizable sphere, with a central point charge generating an electrostatic field obeying Coulomb's Law.
(b) The solvent is a continuous medium, characterized by a polarization field (dipole moment density). Solvent dipoles interact according to Coulomb's Law.
(c) The dielectric response of the solvent is linear and isotropic. In other words, the polarization field is propor-

[a]Corresponding author; Phone: (619) 534-2798; electronic mail: nbaker@wasabi.ucsd.edu

tional to the electrostatic field by a factor $\epsilon_0(\epsilon-1)$, where ϵ_0 is the dielectric permittivity of a vacuum and ϵ is the relative permittivity of the solvent.

Ionic hydration free energies calculated using the Born model and ionic radii derived from crystal structures of ionic compounds, while qualitatively correct, are usually not in quantitative agreement with experiment.[11,42,43] This inaccuracy is due, in part, to the description of the solvent in terms of a continuum (B), an approximation which fails at small distances from the ions where the finite size, covalent geometry, and charge distribution of the solvent molecule become important.

Unlike the Born model, explicit solvent simulations can accurately represent the detailed microscopic structure of the solvent. Nevertheless, these simulations also often fail to give reliable and reproducible solvation free energies[21] unless special care is taken to correct the calculated results.[9,18,43–46] This failure is partly due to the approximate treatment of electrostatic interactions during the simulation. Whether calculated by lattice sum or cutoff-truncation methods, these interactions correspond to an ''effective potential,'' rather than the ''true'' Coulomb potential. To benefit from the accurate microscopic description provided by molecular simulations, the simulation results must be corrected for the approximate nature of the specific effective potential employed during the simulation. One approach for estimating such a correction is to construct a continuum model analogous to the Born model, but involving the modification of hypotheses A and B (see above) to replace the exact Coulomb potential by the effective potential used in the simulation. Comparison of this model with the original Born model leads to a correction which is exact in the limit of continuum electrostatics (infinitesimal dipoles, linear response) and a good approximation when applied to molecular simulations. This method was first used by Neumann for pure water[14,15] and later applied to ion solvation studies to determine corrections to free energies from simulations using truncated Coulomb interactions[18] as well as lattice-sum methods.[9,12,13]

The present study generalizes these types of corrections to effective potentials defined by two arbitrary truncated polynomials governing the ion–solvent and solvent–solvent interactions. The polynomial forms are general enough to encompass most effective potentials currently employed in molecular simulations, such as shifting functions and reaction-field corrections.

Section II develops an integral equation governing the polarization around the ion based on electrostatic interactions defined by these arbitrary truncated polynomials. The first steps of this derivation closely parallel the work of Wood.[18] The integral equation can be solved numerically by two methods detailed in Appendices B and C. Based on this integral equation, an optimal effective potential is determined by a variational fit to the Born polarization. In Sec. III, the results of Sec. II are used to determine the polarization around the ion corresponding to several effective potentials and to the optimal effective potential. Both the polarization and the calculated solvation free energies are compared with the ideal Born result. The comparison of the free energies leads to corrections that may be used directly in molecular simulations. Finally, Sec. IV summarizes the results of this work and its implications.

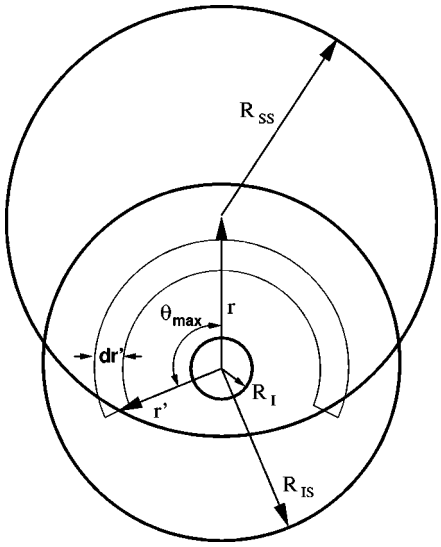

FIG. 1. Illustration of the coordinates and cutoffs used to determine the integral equation for the polarization. The ion, of radius R_I, is located at the center of the coordinate system. Interactions between the ion and solvent are truncated at a distance R_{IS}, while interactions within the solvent are truncated at R_{SS}. This illustrates how the field at $\mathbf{r}$ (along the z axis), due to a shell of solvent of thickness dr' at distance r', is calculated over the angular range 0 to θ_{max}.

II. THEORY

In this section, an integral equation (32) is derived for the ''charge-scaled'' radial polarization $p(r)$ around a spherical ion immersed in a continuum solvent where ion-solvent and solvent-solvent interactions are described by the arbitrary truncated polynomial potentials ϕ_I and ϕ_S. The integral equation is developed by considering an ion of charge q_I and radius R_I at the origin of a spherical coordinate system as shown in Fig. 1. The vectors $\mathbf{r}\equiv(r,\theta,\varphi)$ and $\mathbf{r}'\equiv(r',\theta',\varphi')$ denote arbitrary positions in this coordinate system. An expression (39) is also derived for the solvation free energy ΔG_{solv} based on the solution of the integral equation.

A. General forms of the ion–solvent and solvent–solvent effective potentials

The effective potential at $\mathbf{r}$ due to the ion charge at the origin is assumed to be of the general form

$$\phi_I(r)=\frac{q_I}{4\pi\epsilon_0}H(R_{IS}-r)f_I(r), \tag{1}$$

where $H(x)$ is the Heaviside step function (i.e., unity when $x>0$ and zero otherwise[47]), $R_{IS}>0$ is the ion–solvent interaction cutoff radius, and f_I is a (finite) polynomial

$$f_I(r)\equiv\sum_{k\geqslant -1} a_k r^k \quad \text{with} \quad a_{-1}=1. \tag{2}$$

The coefficients for this polynomial have the units $(\text{length})^{-1-k}$. For a finite value of R_{IS}, the potential defined in (1) satisfies two physical requirements

$$\lim_{r\to\infty}\phi_{\mathrm{I}}(r)=0 \quad \text{and} \quad \lim_{r\to 0}\left[\phi_{\mathrm{I}}(r)-\frac{q_{\mathrm{I}}}{4\pi\epsilon_0 r}\right]=0. \tag{3}$$

In other words, the potential vanishes at infinity and behaves according to Coulomb's law at short distances. Due to the spherical symmetry of the system, the field corresponding to this potential is radial with a magnitude given by

$$E_{\mathrm{I}}(r)=-\frac{q_{\mathrm{I}}}{4\pi\epsilon_0}H(R_{\mathrm{IS}}-r)f_{\mathrm{I}}'(r)+\frac{q_{\mathrm{I}}}{4\pi\epsilon_0}\times\delta(R_{\mathrm{IS}}-r)f_{\mathrm{I}}(r), \tag{4}$$

where $f_{\mathrm{I}}'=df_{\mathrm{I}}/dr$. In a Monte Carlo (MC) simulation, sampling is performed using an energy-based criterion and the relevant truncated quantity is the effective electrostatic potential used during the simulation. Therefore, Eqs. (1) and (4) are exact for this simulation method. However, in a molecular dynamics (MD) simulation, sampling is performed using the force on each particle and the relevant truncated quantity is the effective electrostatic field. Because it operates on an infinitesimally narrow range of distance, the second term of (4) cannot be incorporated when simulating the dynamics of a system and must be omitted. This omission is correct only if $f_{\mathrm{I}}(R_{\mathrm{IS}})=0$ or, in other words, if $\phi_{\mathrm{I}}(r)$ is continuous at R_{IS}. Any function that does not satisfy this condition cannot be sampled by MD. In particular, the choice $f_{\mathrm{I}}(r)=r^{-1}$, corresponding to the ''truncated Coulomb potential,'' is not appropriate for molecular dynamics. In reality, an MD simulation with ''truncated Coulomb forces'' implicitly uses a potential of the form of (1) with $f_{\mathrm{I}}(r)=r^{-1}-R_{\mathrm{IS}}^{-1}$. Although the restriction $f_{\mathrm{I}}(R_{\mathrm{IS}})=0$ does not necessarily apply to MC simulations, it will be imposed in the subsequent discussion with no loss of generality (see Sec. II E). With this condition satisfied, (4) can be rewritten as

$$E_{\mathrm{I}}(r)=-\frac{q_{\mathrm{I}}}{4\pi\epsilon_0}H(R_{\mathrm{IS}}-r)f_{\mathrm{I}}'(r). \tag{5}$$

Likewise, the effective potential at a distance ρ from a solvent charge q_{S} is assumed to be of the general form

$$\phi_{\mathrm{S}}(\rho)=\frac{q_{\mathrm{S}}}{4\pi\epsilon_0}H(R_{\mathrm{SS}}-\rho)f_{\mathrm{S}}(\rho), \tag{6}$$

where $R_{\mathrm{SS}}>0$ is the solvent–solvent interaction cutoff and f_{S} is a (finite) polynomial

$$f_{\mathrm{S}}(\rho)\equiv\sum_{l\geqslant -1} b_l\rho^l \quad \text{with} \quad b_{-1}=1. \tag{7}$$

Like before, the units of the coefficients b_l are $(\text{length})^{-1-l}$. As above, the condition $f_{\mathrm{S}}(R_{\mathrm{SS}})=0$ ensures continuity of the potential at R_{SS} as required by MD simulations. Finally, note that imposing $f_{\mathrm{I}}(R_{\mathrm{IS}})=f_{\mathrm{S}}(R_{\mathrm{SS}})=0$ is equivalent to requiring the dependence of a_0 and b_0 on the other coefficients in the polynomial, namely,

$$a_0=-\sum_{k\neq 0} a_k R_{\mathrm{IS}}^k \quad \text{and} \quad b_0=-\sum_{l\neq 0} b_l R_{\mathrm{SS}}^l. \tag{8}$$

B. Radial component of the field due to a radially oriented solvent point dipole

An expression for the radial component of the electrostatic field generated at $\mathbf{r}$ by a radially oriented solvent point dipole $\boldsymbol{\mu}$ at $\mathbf{r}'$ can be derived based on the potential of a solvent point charge defined in (6). For simplicity, the vector $\mathbf{r}$ is assumed lie along the z axis (see Fig. 1). Only the radial component of the field is relevant because spherical symmetry causes tangential components to cancel upon integration (see Sec. II D). The radial component of the field is equal to the radial derivative of the potential $\phi(\mathbf{r})$ due to the point dipole $\boldsymbol{\mu}$ at $\mathbf{r}'$. The dipoles are defined in the usual manner[48] as two point charges q and $-q$ aligned along the vector $\boldsymbol{\mu}$ and separated by a distance a. The point dipole represents the limits $a\to 0$ and $q\to\infty$ under the constraint $\mu=qa$. Defining $\mathbf{n}\equiv\boldsymbol{\mu}/\mu$, the position of the positive and negative charges are, respectively, $\mathbf{r}'+(a/2)\mathbf{n}$ and $\mathbf{r}'-(a/2)\mathbf{n}$. Using Eq. (6), the corresponding potential $\phi(\mathbf{r})$ is

$$\phi(\mathbf{r})=\frac{q}{4\pi\epsilon_0}\left[H\left(R_{\mathrm{SS}}-\left\|\mathbf{r}-\mathbf{r}'-\frac{a}{2}\mathbf{n}\right\|\right)f_{\mathrm{S}}\left(\left\|\mathbf{r}-\mathbf{r}'-\frac{a}{2}\mathbf{n}\right\|\right)-H\left(R_{\mathrm{SS}}-\left\|\mathbf{r}-\mathbf{r}'+\frac{a}{2}\mathbf{n}\right\|\right)f_{\mathrm{S}}\left(\left\|\mathbf{r}-\mathbf{r}'+\frac{a}{2}\mathbf{n}\right\|\right)\right]. \tag{9}$$

A Taylor expansion around $a=0$ leads to

$$\phi(\mathbf{r})=\frac{qa}{4\pi\epsilon_0}[-H(R_{\mathrm{SS}}-\|\mathbf{r}-\mathbf{r}'\|)\mathbf{n}\cdot\nabla' f_{\mathrm{S}}(\|\mathbf{r}-\mathbf{r}'\|)+\delta(R_{\mathrm{SS}}-\|\mathbf{r}-\mathbf{r}'\|)f_{\mathrm{S}}(\|\mathbf{r}-\mathbf{r}'\|)\mathbf{n}\cdot\nabla'\|\mathbf{r}-\mathbf{r}'\|]+\mathcal{O}(a^3). \tag{10}$$

Since $f_{\mathrm{S}}(R_{\mathrm{SS}})=0$, the delta term in this expression vanishes. Considering the limits $a\to 0$, $q\to\infty$ and using $\mu=qa$, this expression can be rewritten as

$$\phi(\mathbf{r})=-\frac{\mu}{4\pi\epsilon_0}\left[H(R_{\mathrm{SS}}-\|\mathbf{r}-\mathbf{r}'\|)\mathbf{n}\cdot\frac{\mathbf{r}-\mathbf{r}'}{\|\mathbf{r}-\mathbf{r}'\|}\times f_{\mathrm{S}}'(\|\mathbf{r}-\mathbf{r}'\|)\right]. \tag{11}$$

For a radially oriented solvent dipole, $\mathbf{n}=\mathbf{r}'/r$. Since $\mathbf{r}$ is aligned with the z axis of the coordinate system, the angle between $\mathbf{r}$ and $\mathbf{r}'$ is simply θ' and (11) can be rewritten as

$$\phi(r,r',\theta')=\frac{\mu}{4\pi\epsilon_0}H(R_{\mathrm{SS}}-\|\mathbf{r}-\mathbf{r}'\|)f_{\mathrm{S}}'(\|\mathbf{r}-\mathbf{r}'\|)\times\frac{r'-r\cos\theta'}{\sqrt{r^2+r'^2-2rr'\cos\theta'}}, \tag{12}$$

where the relations $[-(\mathbf{r}-\mathbf{r}')\cdot\mathbf{r}']/r'=r'-r\cos\theta'$ and $\|\mathbf{r}-\mathbf{r}'\|=\sqrt{r^2+r'^2-2rr'\cos\theta'}$ were used. Inserting the definition of f_{S} from (7) gives

$$\phi(r,r',\theta')=\frac{\mu}{4\pi\epsilon_0}H(R_{\mathrm{SS}}-\|\mathbf{r}-\mathbf{r}'\|)\sum_l b_l\phi_l(r,r',\theta') \tag{13}$$

with

$$\phi_l(r,r',\theta')=l(r'-r\cos\theta')\times(r^2+r'^2-2rr'\cos\theta')^{l/2-1}. \tag{14}$$

The radial component of the field at $\mathbf{r}$ is given by the negative derivative of (13) with respect to r

$$E_r(r,r',\theta') = \frac{\mu}{4\pi\epsilon_0}\Bigg[H(R_{SS}-\|\mathbf{r}-\mathbf{r}'\|) \times \sum_l b_l E_{rl}(r,r',\theta') + \frac{r'-r\cos\theta'}{\sqrt{r^2+r'^2-2rr'\cos\theta'}} \times \delta(R_{SS}-\|\mathbf{r}-\mathbf{r}'\|)\sum_l b_l \phi_l(r,r',\theta')\Bigg] \quad (15)$$

with

$$E_{rl}(r,r',\theta') = -\frac{\partial\phi_l(r,r',\theta')}{\partial r} = l(r^2+r'^2-2rr'\cos\theta')^{l/2-2} \times [(l-1)(r^2+r'^2)\cos\theta' - (l-2)rr' - lrr'\cos^2\theta']. \quad (16)$$

This expression diverges for $r=r'$, $\theta'=0$ when $l=\pm 1$. In the following, Eq. (15) will always be used with $\|\mathbf{r}-\mathbf{r}'\| < R_{SS}$. In this case, the delta function term can be omitted.

C. Radial component of the field due to a radially polarized volume element of solvent

This section introduces a continuous description of the solvent through the polarization vector $\mathbf{P}(\mathbf{r}')$. Consider the volume element $dV'=r'^2dr'\sin\theta' d\theta' d\varphi'$ of the solvent at $\mathbf{r}'\equiv(r',\theta',\varphi')$. The dipole moment $d\boldsymbol{\mu}$ of this volume element is related to the polarization $\mathbf{P}(\mathbf{r}')$ at $\mathbf{r}'$ through

$$d\boldsymbol{\mu}(\mathbf{r}') = \mathbf{P}(\mathbf{r}')dV' = \mathbf{P}(\mathbf{r}')r'^2dr'\sin\theta' d\theta' d\varphi'. \quad (17)$$

Due to the spherical symmetry of the system, both the dipole and the polarization vectors are radially oriented and independent of the angular degrees of freedom. These quantities have magnitudes $d\mu(r')$ and $P(r')$, respectively. Using the continuum representation introduced in (17), the radial component of the field at $\mathbf{r}$ induced by a dipole $d\boldsymbol{\mu}$ in the volume element dV' at $\mathbf{r}'$ can be written as

$$dE_r(r,r',\theta';dV') = \frac{1}{4\pi\epsilon_0}P(r')r'^2dr'\sin\theta' d\theta' d\varphi' \times H(R_{SS}-\|\mathbf{r}-\mathbf{r}'\|)\sum_l b_l E_{rl}(r,r',\theta'), \quad (18)$$

where (15) was used with $\|\mathbf{r}-\mathbf{r}'\|<R_{SS}$. However, this expression neglects the singularities in $E_{rl}(r,r',\theta')$ for $l=\pm 1$ when $r=r'$, $\theta'=0$ and must be appropriately corrected.

It is well known that the discontinuity in the Coulomb potential ($b_l=0$ for all $l\neq -1$, $R_{SS}\to\infty$) across dV' from $\mathbf{r}'-\mathbf{r}'dr'/(2r')$ to $\mathbf{r}'+\mathbf{r}'dr'/(2r')$ is given by[48,49]

$$\Delta\phi = \frac{1}{\epsilon_0}P(r')dr'. \quad (19)$$

Since there is no such potential discontinuity for $l=1$, no correction needs to be made in this case. Thus, the correction to $dE_r(r,r',\theta';dV')$ due to singularities at $r=r'$, $\theta'=0$ is simply

$$dE_r^{\mathrm{corr}}(r,r',\theta';dV') = -\frac{1}{\epsilon_0}P(r')\delta(r-r') \times \delta(\theta')\delta(\varphi')dr'd\theta'd\varphi'. \quad (20)$$

Equation (20) expresses the fact that the discontinuity in $E_{r,-1}(r,r',\theta';dV')$ is integrable. It can be shown that terms in (7) with $l<-1$ would lead to nonintegrable discontinuities. Therefore, the restriction of the series for f_S to $l\geqslant -1$ is a necessary condition for developing the present continuum formalism.

D. Field generated by a radially polarized shell of solvent

The next step is to determine the field at $\mathbf{r}$ arising from a solvent shell of thickness dr' at a distance r' (see Fig. 1). To calculate the magnitude of this field, Eq. (18) corrected by (20) is integrated over the surface of a solvent shell. Due to the symmetry of the shell around the z axis, the field generated at $\mathbf{r}$ is radial. The magnitude of this field, obtained by integration of the radial field over θ' and φ', is

$$dE(r,r';dr') = \frac{P(r')}{\epsilon_0}\Bigg[\sum_{l\geqslant -1} b_l I_l(r,r') - \delta(r-r')\Bigg]dr', \quad (21)$$

where the δ function term arises from the correction $dE_r^{\mathrm{corr}}(r,r',\theta')$ given in (20) and

$$I_l(r,r') \equiv \frac{r'^2}{2}\int_0^{\theta_{\max}} E_{rl}(r,r',\theta')\sin\theta' d\theta'. \quad (22)$$

The integral over φ' in (21) is trivial and gives a factor of 2π. The upper limit on the integral over θ', $\theta_{\max} \equiv \theta_{\max}(r,r';R_{SS},R_{IS})$, is defined as the maximum angle θ' in the range $(0,\pi)$ for which $H(R_{SS}-\|\mathbf{r}-\mathbf{r}'\|)=1$ (see Fig. 1)

$$\theta_{\max} = \begin{cases} \pi & r'+r\leqslant R_{SS} \\ 0 & |r'-r|\geqslant R_{SS} \\ \cos^{-1}\left(\dfrac{r'^2+r^2-R_{SS}^2}{2r'r}\right) & \text{otherwise.} \end{cases} \quad (23)$$

When (16) and (23) are inserted into (22), the integral becomes

$$I_l(r,r') = \begin{cases} 0 & r'+r\leqslant R_{SS} \text{ or } |r'-r|\geqslant R_{SS} \\ \Psi_l(r,r') & \text{otherwise,} \end{cases} \quad (24)$$

where

$$\Psi_l(r,r') \equiv \frac{l}{8(l+2)r^2}[-2(l+2)R_{SS}^{l}(r^2+r'^2) - l(l+2)R_{SS}^{l-2}(r^2-r'^2)^2+4(l+1) \times (r^2+lrr'+r'^2)(r-r')^l+l^2R_{SS}^{l+2}]. \quad (25)$$

Using this result with (21) and $b_{-1}=1$, the field can finally be written as

$$dE(r,r';dr') = \frac{P(r')}{\epsilon_0}dr' \times \begin{cases} -\delta(r'-r) & r+r' \leqslant R_{SS} \text{ or } |r'-r| \geqslant R_{SS} \\ \Sigma_{l\geqslant -1} b_l \Psi_l(r,r') - \delta(r'-r) & \text{otherwise.} \end{cases} \quad (26)$$

E. Integral equation defining the radial polarization around the ion

Equations in continuum electrostatics are usually developed under the assumption of a linear relationship between the polarization and the field in the dielectric continuum. Following Neumann,[14] the polarization can be related to the electrostatic field by

$$\mathbf{P}(\mathbf{r}) = \epsilon_0(\epsilon-1)\mathbf{E}(\mathbf{r}) = \epsilon_0(\epsilon-1)\left[\mathbf{E}_I(\mathbf{r}) + \int \mathsf{T}(\mathbf{r}-\mathbf{r}')\mathbf{P}(\mathbf{r}')d\mathbf{r}'\right], \quad (27)$$

where $\mathsf{T}(\mathbf{r})$ is a modified dipole–dipole interaction tensor. Since both the polarization and field vectors are radial and the ion is nonpolarizable, this relationship can be written in scalar form as

$$P(r) = \begin{cases} 0 & r \leqslant R_I \\ \epsilon_0(\epsilon-1)E(r) & r > R_I, \end{cases} \quad (28)$$

where ϵ_0 is the vacuum permittivity and ϵ is the relative permittivity of the dielectric continuum. The field $E(r)$ is a sum of $E_I(r)$ from the ion and contributions from the solvent dipole shells, which are obtained by integrating the field generated by each shell, $dE(r,r';dr')$, over r'

$$E(r) = E_I(r) + \int_{R_I}^{\infty} dE(r,r';dr'). \quad (29)$$

Inserting (5), (26), and (28) gives

$$P(r) = -\frac{q_I(\epsilon-1)}{4\pi\epsilon}H(R_{IS}-r)f_I'(r) + \frac{(\epsilon-1)}{\epsilon}\int_{v(r)}^{w(r)} P(r')\sum b_l\Psi_l(r,r')dr' \quad (30)$$

for $r \geqslant R_I$, where

$$v(r) = \max(R_I, |r-R_{ss}|),$$
$$w(r) = R_{ss}+r. \quad (31)$$

By comparing (30) and (27), it can be seen that the sum over Ψ_l under the integral can be related to the modified dipole-dipole interaction tensor $\mathsf{T}(\mathbf{r})$.

Noting that $P(r)$ is linearly related to q_I in (30), a charge-scaled polarization, independent of charge, is defined as $p(r)=P(r)/q_I$. The integral equation (30) can be recast into a more general form

$$p(r) = g(r) + \lambda\int_{v(r)}^{w(r)} K(r,r')p(r')dr' \quad \text{for } r \geqslant R_I, \quad (32)$$

which is an inhomogeneous linear integral equation.[50] Note that this equation is only valid for $r \geqslant R_I$; for smaller values of r, (28) implies $p(r)=0$. The ''eigenvalue'' of Eq. (32) is related to the solvent permittivity

$$\lambda = \frac{\epsilon-1}{\epsilon}, \quad (33)$$

while the inhomogeneous term $g(r)$ is related to the electrostatic field caused by the ion

$$g(r) = \frac{\epsilon_0\lambda}{q_I}E_I(r) = -\frac{\lambda}{4\pi}H(R_{IS}-r)\sum_{k\geqslant -1} k a_k r^{k-1}. \quad (34)$$

Finally, the kernel of the integral equation is related to the solvent-solvent interaction polynomial from Eq. (25) by

$$K(r,r') = \sum_{l\geqslant -1} b_l\Psi_l(r,r'). \quad (35)$$

To be valid, this Eq. (32) must yield the Born polarization

$$p_{Born}(r) = \frac{\lambda}{4\pi r^2} \quad (36)$$

as its solution in the limits $R_{IS}\to\infty$ and $R_{SS}\to\infty$ for a Coulomb potential ($a_k=0$ for all $k\neq -1$, $b_l=0$ for all $l\neq -1$). This limit is demonstrated in Appendix A. Integral equations such as (32) can be solved using either numerical or approximate analytical methods as detailed in Appendices B and C.

It is interesting to note that for certain choices of f_S, the kernel may be zero. In these cases, the behavior of the polarization is completely controlled by the interaction function chosen for the ion–solvent potential, namely, $p(r)=g(r)$. For example, such a situation is encountered when $f_S(r) = r^{-1}+r^2R_{SS}^{-3}/2-3R_{SS}^{-1}/2$ (see Sec. III B). It is also worth noting that since $\Psi_0=0$ in Eq. (35) and since only f_I' is involved in (32), neither a_0 nor b_0 have influence on $p(r)$. Therefore, imposing the continuity restrictions $f_I(R_{IS})=0$ and $f_S(R_{SS})=0$ has no consequences for the polarization.

F. Relation between polarization and solvation free energy

If Eq. (32) can be solved for $p(r)$, this quantity can be used to determine ΔG_{solv}, the ionic solvation free energy corresponding to the specific effective potential. This free energy can then be compared to the Born solvation free energy ΔG_{Born} corresponding to the ideal case of nontruncated electrostatics[41]

$$\Delta G_{Born} = -\frac{q_I^2(\epsilon-1)}{8\pi\epsilon_0\epsilon R_I}. \quad (37)$$

This comparison can be used to assess the perturbation to the solvation free energy induced by the use of the interaction

potentials ϕ_I and ϕ_S instead of a Coulomb potential. The potential at the center of an ion of charge q is given from $p(r)$ by multiplying by q and integrating the continuous analog of (13) over space, using f_I instead of f_S,

$$\phi(r=0;q)=\frac{q}{\epsilon_0}\sum_{k\geqslant -1} ka_k\int_{R_I}^{R_{IS}} p(r')r'^{k+1}dr'. \tag{38}$$

The free energy for reversibly charging the ion is

$$\Delta G_{solv}=\int_0^{q_I}\phi(r=0;q)dq$$

$$=\frac{q_I^2}{2\epsilon_0}\sum_{k\geqslant -1} ka_k\int_{R_I}^{R_{IS}} p(r')r'^{k+1}dr'. \tag{39}$$

Since $p(r)$ is independent of a_0 and b_0 and due to the form of (39), ΔG_{solv} is also independent of these constants. Finally, the ionic solvation free energy result obtained from (39) can be used to determine a correction ΔG_{corr} for the truncated electrostatic interactions by comparison with the Born free energy

$$\Delta G_{corr}=\Delta G_{Born}-\Delta G_{solv}=\Delta G_{corr}^{in}+\Delta G_{corr}^{out}. \tag{40}$$

The correction due to modification of the polarization inside R_{IS} is

$$\Delta G_{corr}^{in}=-\frac{q_I^2(\epsilon-1)}{8\pi\epsilon_0\epsilon}\left(\frac{1}{R_I}-\frac{1}{R_{IS}}\right)-\Delta G_{solv} \tag{41}$$

and the correction due to the neglect of interactions with the polarization outside R_{IS} is

$$\Delta G_{corr}^{out}=-\frac{q_I^2(\epsilon-1)}{8\pi\epsilon_0\epsilon R_{IS}}. \tag{42}$$

ΔG_{corr}^{in} and ΔG_{corr}^{out} are the generalized forms of the corrections C_{ss} and C_{is} proposed by Wood.[18]

The free energy integral (39) can be evaluated numerically by a simple quadrature [see Eq. (C5)] or determined from approximate analytical solutions such as Neumann series [see Eq. (B11)]. However, in the special cases where the kernel vanishes (see Sec. III B), exact analytical expressions are obtained

$$\Delta G_{solv}=-\frac{q_I^2(\epsilon-1)}{8\pi\epsilon_0\epsilon}\sum_{k\geqslant -1}\sum_{k'\geqslant -1}\frac{kk'a_ka_{k'}}{k+k'+1}$$

$$\times(R_{IS}^{k+k'+1}-R_I^{k+k'+1}), \tag{43}$$

$$\Delta G_{corr}^{in}=\frac{q_I^2(\epsilon-1)}{8\pi\epsilon_0\epsilon}\sum_{k\geqslant 1}\sum_{k'\geqslant 1}\frac{kk'a_ka_{k'}}{k+k'+1}$$

$$\times(R_{IS}^{k+k'+1}-R_I^{k+k'+1}). \tag{44}$$

G. The optimal effective potential

The integral equation (32) can be used to find the functions f_I and f_S that give the best agreement between the calculated polarization and the Born result from Eq. (36) on either side of the ion–solvent electrostatic cutoff point. To accomplish this optimization, Eq. (32) must be solved for the best choices of the a_k and b_l coefficients using the Born polarization for $p(r)$

$$\frac{1}{r^2}=-H(R_{IS}-r)\left[\sum_{k\geqslant -1}^{K} ka_kr^{k-1}\right]$$

$$+\lambda\int_{v(r)}^{w(r)} r'^{-2}\sum_{l\geqslant -1}^{L} b_l\Psi_l(r,r')dr'. \tag{45}$$

For a finite polynomial, the integral over r' can be taken inside the sum over l. Defining

$$\Lambda_l(r)\equiv\lambda r^2\int_{v(r)}^{w(r)} r'^{-2}\Psi_l(r,r')dr'$$

$$=\frac{\lambda l}{4(l+2)v}\Bigg\{2[(l+1)r+v](r-v)^{l+1}$$

$$-R_{SS}^l[(l+2)(r^2-v^2)+lR_{SS}^2]-\frac{l(l+2)R_{SS}^{l-2}}{6}$$

$$\times(3r^4-8r^3v+6r^2v^2-v^4+4R_{SS}^3v-3R_{SS}^4)$$

$$-4R_{SS}^{l+2}\delta_{(-1)^l,-1}v\frac{(l+2)r+R_{SS}}{r+R_{SS}}\Bigg\}, \tag{46}$$

where $v\equiv v(r)$ and $\delta_{i,j}$ is the Kronecker delta symbol,[47] allows (45) to be expressed as

$$\rho(r)=1+H(R_{IS}-r)\left[\sum_{k\geqslant -1}^{K} ka_kr^{k+1}\right]$$

$$-\left[\sum_{l\geqslant -1}^{L} b_l\Lambda_l(r)\right]=0. \tag{47}$$

This equation must be solved for the optimal values of a_k and b_l in a least-squares sense. The best solution over an interval (r_i,r_f), has a minimum residual

$$\chi=\frac{1}{2}\int_{r_i}^{r_f}\rho^2(r)dr. \tag{48}$$

Therefore, the equations

$$\frac{\partial\chi}{\partial a_k}=k\int_{r_i}^{r_f} r^{k+1}H(R_{IS}-r)\rho(r)dr=0 \quad \text{and}$$

$$\frac{\partial\chi}{\partial b_l}=-\int_{r_i}^{r_f}\Lambda_l(r)\rho(r)dr=0 \tag{49}$$

must be solved for every k and l. Not surprisingly, these equations are automatically satisfied for $k=0$ and $l=0$. Therefore, the choice of a_0 and b_0 is arbitrary and the potential continuity constraints $f_S(R_{SS})=f_I(R_{IS})=0$ can be satisfied without affecting the performance of the optimization.

Inserting the definition of $\rho(r)$ from (47) and assuming $R_{IS}\in(r_i,r_f)$, the equations can be written as

$$\sum_{k'\geqslant -1}^{K} k'A(k,k')a_{k'}-\sum_{l'\geqslant -1}^{L} B(k,l')b_{l'}=-A(k,-1),$$

$$k=-1,1,2,3,\ldots,K, \tag{50}$$

$$\sum_{k'\geqslant -1}^{K} k'B(k',l)a_{k'} - \sum_{l'\geqslant -1}^{L} C(l,l')b_{l'} = -B(-1,l),$$

$$l = -1,1,2,3,\ldots,L. \quad (51)$$

The coefficients are given by

$$A(k,k') \equiv \int_{r_i}^{R_{IS}} r^{k+k'+2}dr, \quad B(k,l) \equiv \int_{r_i}^{R_{IS}} r^{k+1}\Lambda_l(r)dr,$$

$$C(l,l') \equiv \int_{r_i}^{r_f} \Lambda_l(r)\Lambda_{l'}(r)dr, \quad D(l) \equiv \int_{R_{IS}}^{r_f} \Lambda_l(r)dr. \quad (52)$$

Furthermore, b_{-1} and a_{-1} should be restricted to values of 1. This simply reflects the desire to have the potential behave as Coulomb's Law at short distances. Specifically, this means solving the new system of equations

$$\sum_{k'\geqslant 1}^{K} k'A(k,k')a_{k'} - \sum_{l'\geqslant 1}^{L} B(k,l')b_{l'} = B(k,-1),$$

$$k = 1,2,\ldots,K, \quad (53)$$

$$\sum_{k'\geqslant 1}^{K} k'B(k',l)a_{k'} - \sum_{l'\geqslant 1}^{L} C(l,l')b_{l'} = C(l,-1) - D(l),$$

$$l = 1,2,\ldots,L. \quad (54)$$

It can be expected that the optimum values of the coefficients should depend on R_I, R_{IS}, R_{SS}, and ϵ.

These equations can be solved numerically for all cases.[51] However, due to the complexity of $v(r)$ in (46), this system is amenable to a simple analytical solution only when the ionic radius R_I is set to zero. This approximation, which implies that the ion has the same polarizability as the solvent, is reasonable for small ions. By simple linear algebra techniques, it can be seen that, under the assumption $R_I \to 0$, the system of equations ceases to be linearly independent for the inclusion of polynomial terms larger than second order in either f_I or f_S. Including such higher order terms yields families of solutions with identical values of χ. Since these families contain one solution where each of the higher order coefficients is zero, the second order interaction polynomials are the simplest optimal choice. Moreover, when the optimization is performed for $f_I(r) = r^{-1} + a_0 + a_1 r + a_2 r^2$ and $f_S(r) = r^{-1} + b_0 + b_1 r + b^2 r^2$, the optimal coefficients are independent of r_i and r_f, provided that $r_i \leqslant R_{IS} \leqslant r_f$. Upon solution of the system of equations with *Mathematica*,[52] the optimum coefficients are

$$a_1 = b_1 = 0, \quad a_2 = \frac{1}{2R_{SS}^3}, \quad b_2 = -\frac{2+\epsilon}{4R_{SS}^3(\epsilon-1)}, \quad (55)$$

which are independent of R_{IS} and, in the limit of a high dielectric medium, of ϵ. Using $f_S(R_{SS}) = f_I(R_{IS}) = 0$ gives

$$a_0 = -\frac{1}{R_{IS}} - \frac{R_{IS}^2}{2R_{SS}^3}, \quad b_0 = -\frac{1}{R_{SS}} + \frac{2+\epsilon}{4R_{SS}(\epsilon-1)}. \quad (56)$$

Therefore, the optimum polynomial function, under the assumption $R_I \to 0$, treats the ion–solvent and solvent–solvent interactions differently.

III. COMPARISONS OF SEVERAL COMMON EFFECTIVE POTENTIALS

This section uses Eq. (32) to examine the polarization and solvation free energy corresponding to several schemes commonly used in molecular simulations with truncated electrostatic interactions. These are then compared to the Born polarization from Eq. (36) and solvation free energy from Eq. (37), which are the exact results within the limits of continuum electrostatics.

A. Truncated Coulomb interaction

The most easily implemented truncation scheme is the Coulomb potential with a cutoff. This corresponds to using the interaction polynomials $f_I(r) = r^{-1} - R_{IS}^{-1}$ and $f_S(r) = r^{-1} - R_{SS}^{-1}$. The kernel for the integral equation can be written as

$$K(r,r') = \Psi_{-1}(r,r') - \frac{\Psi_0(r,r')}{R_{SS}}$$

$$= \frac{1}{8r^2}[-2R_{SS}^{-1}(r^2+r'^2) + R_{SS}^{-3}(r^2-r'^2)^2 + R_{SS}], \quad (57)$$

using (25), (35), and $\Psi_0 = 0$. The inhomogeneous term for the integral equation is

$$g(r) = \frac{\lambda}{4\pi r^2} H(R_{IS}-r) = p_{Born}(r)H(R_{IS}-r), \quad (58)$$

where λ is given by (33) and $p_{Born}(r)$ by (36). The Nystrom method of Appendix C is used to solve (32). Figures 2(a) and 2(b) show the charge-scaled polarization $p(r)$ due to this truncated interaction with $\epsilon = 78$ (water) and $R_I = 0.2$ nm (approximately the radius of a Na^+ ion). Figure 2(c) presents the first three Neumann series analytical approximations calculated as described in Appendix B.

In all cases, the curves are discontinuous at R_{IS}. Furthermore, the polarization below R_{IS} is consistently larger than predicted by the Born model, whereas the polarization above is smaller, although always positive. With $R_{IS} = R_{SS}$ [Fig. 2(a)], the deviation between $p(r)$ and $p_{Born}(r)$, as well as the magnitude of the discontinuity in $p(r)$, decreases when the cutoff radius is increased. However, even for a cutoff radius of 1.4 nm, the difference is not negligible. When R_{SS} is varied while keeping $R_{IS} = 1.2$ nm [Fig. 2(b)], the positive deviation of $p(r)$ with respect to $p_{Born}(r)$ below R_{IS} diminishes with increasing R_{SS}. On the other hand, the negative deviation of $p(r)$ above R_{IS} increases in magnitude with increasing R_{SS}. For large values of R_{SS}, $p(r)$ becomes close to zero beyond R_{IS}. The magnitude of the discontinuity in $p(r)$ at R_{IS} is only weakly sensitive to R_{SS}. Underpolarization of the solvent above R_{IS} is easily understood since the solvent above this distance does not ''feel'' the electrostatic field due to the ion. Inside the cutoff, the solvent is overpolarized because each solvent volume element only interacts with a fraction of the highly polarized solvent inside the ion cutoff sphere. This partial interaction results in a bias of the polarization of the solvent element towards the ion. As can be seen from Fig. 2(c), the zeroth-order Neumann approxima-

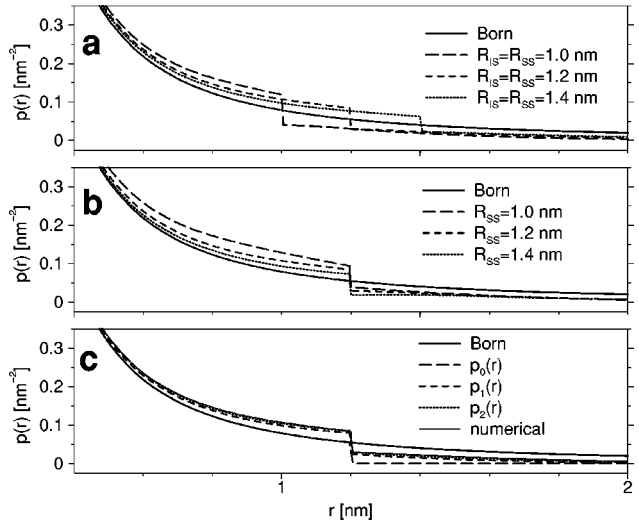

FIG. 2. Charge-scaled polarization $p(r)$ obtained by numerically solving Eq. (32) discretized as (C1) with $\Delta r=0.005$ nm, $R_{\max}=7.0$ nm, $R_I=0.2$ nm, and $\epsilon=78$. The interaction polynomials are $f_I(r)=r^{-1}-R_{IS}^{-1}$ and $f_S(r)=r^{-1}-R_{SS}^{-1}$. (a) Curves corresponding to $R_{IS}=R_{SS}=1.0$, 1.2, and 1.4 nm are represented, together with the Born polarization (36), where $p_{\mathrm{Born}}(R_I)=1.96$. (b) Curves corresponding to $R_{IS}=1.2$ nm and $R_{SS}=1.0$, 1.2, and 1.4 nm. (c) Neumann series approximations p_0, p_1, and p_2 shown together with the Born and numerical results for $R_{IS}=R_{SS}=1.2$ nm, see Eqs. (B8)–(B10).

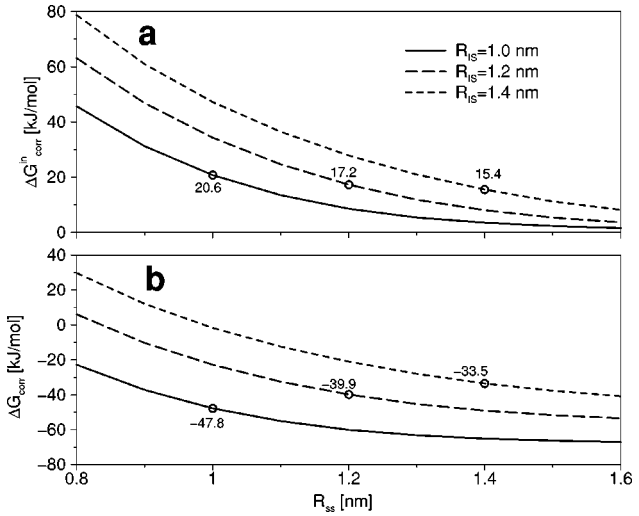

FIG. 3. Corrections $\Delta G^{\mathrm{in}}_{\mathrm{corr}}$ (a) and ΔG_{corr} (b) from Eqs. (40) and (41) for $f_I(r)=r^{-1}-R_{IS}^{-1}$ and $f_S(r)=r^{-1}-R_{SS}^{-1}$ are displayed as functions of R_{SS} for $q_I=+1e$ and $R_{IS}=1.0$, 1.2, and 1.4 nm. $p(r)$ is evaluated numerically as for Figs. 2(a) and 2(b).

tion to $p(r)$ is in poor agreement with the numerical estimate of $p(r)$. However, higher order approximations, such as $p_1(r)$ and $p_2(r)$, converge rapidly to the exact function. The second-order Neumann series approximation thus offers a reasonably accurate analytical correction to the truncation of the Coulombic electrostatic interactions.

For the truncated Coulomb potential, ΔG_{solv} has a very simple interpretation. It is simply the integral of $p(r)$ between R_I and R_{IS} multiplied by $-q_I^2/(2\epsilon_0)$. Correspondingly, $\Delta G^{\mathrm{in}}_{\mathrm{corr}}$ in (41) is proportional to the difference between the integrals evaluated for $p_{\mathrm{Born}}(r)$ and $p(r)$. This quantity is always positive due to the overpolarization effect discussed above. $\Delta G^{\mathrm{out}}_{\mathrm{corr}}$ represents the Born solvation due to solvent shells outside R_{IS}. This term is always negative and depends only on R_{IS}. Figures 3(a) and 3(b) depict $\Delta G^{\mathrm{in}}_{\mathrm{corr}}$ and ΔG_{corr}, respectively, as functions of R_{SS} with $q_I=+1e$ for three values of R_{IS}. As expected from Fig. 2(b), $\Delta G^{\mathrm{in}}_{\mathrm{corr}}$ (and thus ΔG_{corr}, which differs from $\Delta G^{\mathrm{in}}_{\mathrm{corr}}$ only by the R_{IS}-dependent constant $\Delta G^{\mathrm{out}}_{\mathrm{corr}}$) rapidly decreases with R_{SS}. As R_{IS} increases, the curves are shifted upwards because the interval of integration (R_I,R_{IS}) for calculating $\Delta G^{\mathrm{in}}_{\mathrm{corr}}$ increases. Finally, it is interesting to note that if $R_{IS}=R_{SS}$, $\Delta G^{\mathrm{in}}_{\mathrm{corr}}$ is only weakly dependent on the exact cutoff value. The present results are in good agreement with those of Wood[18] for the same truncated Coulomb potential. An analytical expression for the ionic solvation free energy for the second order Neumann correction is presented in Appendix B (B11). Table I lists the solvation free energy values together the Born free energy for the Neumann and numerical treatment of the truncated Coulomb interactions. Notice that, as expected, the Coulomb effective potential underestimates the magnitude of the free energy of solvation for the ion. It is encouraging, however, that the analytical result for this free energy is close to the values obtained by numerical methods, suggesting a possible analytical correction to free energies obtained from simulations using such effective potentials.

TABLE I. Ionic solvation free energies (kJ/mol) for truncated Coulomb as well as Barker and Watts (B&W) interaction potentials. Values in the ''Coulomb (num.)'' and ''B&W (num.)'' columns are evaluated numerically according to the discretization (C1) and quadrature (C5). Column ''Coulomb (p_2)'' contains values corresponding to the second-order Neumann series correction (B10), while column ''B&W (ana.)'' contains values from the analytic expression for the free energy (63). The free energy values are calculated for $q_I=+1e$, $R_I=0.2$ nm, $R_{IS}=R_{SS}=R$ (nm), and $\epsilon=78$. For the numerical estimates, $\Delta r=0.005$ nm and $R_{\max}=7.0$ nm. ΔG_{Born} evaluates to -342.9 kJ/mol.

	Coulomb (num.)		Coulomb (p_2)		B&W (num.)		B&W (ana.)		
R	ΔG_{solv}	$\Delta G^{\mathrm{in}}_{\mathrm{corr}}$	ΔG_{solv}	$\Delta G^{\mathrm{in}}_{\mathrm{corr}}$	ΔG_{solv}	$\Delta G^{\mathrm{in}}_{\mathrm{corr}}$	ΔG_{solv}	$\Delta G^{\mathrm{in}}_{\mathrm{corr}}$	$\Delta G^{\mathrm{out}}_{\mathrm{corr}}$
1.0	−295.1	20.6	−292.7	18.4	−222.2	−52.1	−223.2	−51.1	−68.6
1.2	−303.0	17.2	−301.4	15.6	−241.6	−44.1	−242.5	−43.3	−57.1
1.4	−309.3	15.4	−307.5	13.6	−255.7	−38.2	−256.6	−37.3	−49.0
1.6	−313.4	13.4	−312.2	12.1	−266.4	−33.6	−267.2	−32.9	−42.9
1.8	−317.0	12.2	−315.8	11.0	−274.8	−30.0	−275.5	−29.3	−38.1

B. Barker and Watts reaction field

One of the most common effective potentials used in molecular simulations is the truncated Coulomb potential with the Barker and Watts reaction-field correction.[35] If this form is applied to solvent–solvent interactions,

$$f_S(r)=\frac{1}{r}+\frac{\xi r^2}{2R_{SS}^3}-\frac{\xi+2}{2R_{SS}} \quad \text{with} \quad \xi=\frac{\epsilon-1}{\epsilon+1/2}. \tag{59}$$

Using $\Psi_0=0$, the kernel is written as

$$K(r,r')=\Psi_{-1}(r,r')+\frac{\xi}{2R_{SS}^3}\Psi_2(r,r')-\frac{\xi+2}{2R_{IS}}$$
$$=\frac{1-\xi}{4r^2}[-2R_{SS}^{-1}(r^2+r'^2)+R_{SS}^{-3}(r^2-r'^2)^2+R_{SS}]. \tag{60}$$

When $\xi=1$, $K(r,r')=0$ and (32) has the analytical solution

$$p(r)=g(r)=\frac{\epsilon_0\lambda}{q_I}E_I(r), \tag{61}$$

where $E_I(r)$ is the electrostatic field due to the ion. Thus, with this choice for the solvent–solvent interactions, the polarization in the solvent is directly proportional to the electric field generated by the ion, regardless of the form of this field. In other words, although solvent–solvent interactions are truncated, the reaction-field correction to these interactions exactly compensates for this truncation and the solvent behaves as a homogeneous continuum obeying the exact form of Coulomb's law.

Figure 4 shows $p(r)$ for the Barker and Watts reaction field where

$$f_S(r)=\frac{1}{r}+\frac{\xi r^2}{2R_{IS}^3}-\frac{\xi+2}{2R_{IS}} \quad \text{and} \quad f_I(r)=\frac{1}{r}-\frac{1}{R_{IS}} \tag{62}$$

for a variety of cutoff radii. Because the curves $\epsilon=78$ and $\epsilon\to\infty$ ($\xi=1$) are nearly identical, only one is shown for each cutoff distance. Note that, as mentioned above, the polarization is zero beyond R_{IS}. Furthermore, when the Barker and Watts effective potential is used for the ion–solvent interactions, the polarization is continuous at the cutoff radius. Such continuity is beneficial in simulations, as it prevents artificial heating due to the potential truncation.

Due to the simple form for this polarization function, an analytic form for the free energy of solvation can be obtained. Since the kernel of the integral equation vanishes, the integral for determining the free energy is trivial to evaluate. This is described in general terms in (43); for the specific case given in (62), this energy is

$$\Delta G_{solv}=-\frac{q_I^2(\epsilon-1)}{8\pi\epsilon\epsilon_0}\left(\frac{1}{R_{IS}}-\frac{1}{R_I}\right). \tag{63}$$

This energy is compared to the values obtained by numerical methods in Table I. Notice that, like the Coulomb effective potential, the Barker and Watts potential underestimates the magnitude of the free energy for ionic solvation. For this effective potential, however, the very simple analytical expression for the solvation free energy is exact (in the limit $\xi\to1$). As Table I illustrates, the numerical results agree with the analytical expression within 1% error, suggesting good accuracy for the numerical methods used in this work.

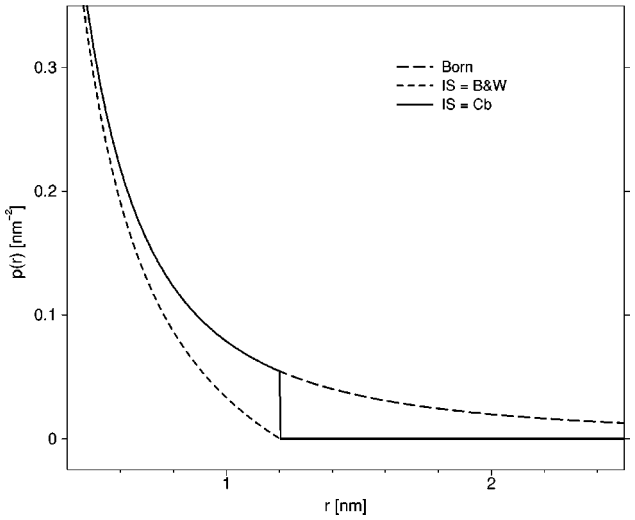

FIG. 4. Charge-scaled polarization for the Barker and Watts reaction-field correction scheme with interaction polynomials f_S and f_I given by (62). The curves correspond to a truncated Coulomb scheme ($f_I=r^{-1}-R_{IS}^{-1}$, labeled IS=Cb) or $f_I=f_S$ (labeled IS=B&W). They are evaluated as for Figs. 2(a) and 2(b) with $R_I=0.2$ nm, $\epsilon=78$, and $R_{IS}=R_{SS}=1.2$ nm. The Born polarization is also displayed.

Another interesting feature of the Barker and Watts reaction-field correction is that when solute-solvent interactions are truncated, the polarization is zero beyond a given distance from the solute. Therefore, in explicit solvent simulations, the effect of artificial periodicity when using this reaction-field correction should be significantly reduced and the system size dependence of calculated ionic solvation free energies should vanish.

One interesting possibility for future work would be an attempt to generalize this result to an arbitrarily shaped cavity and charge distribution. If the exact compensation for truncation of the Barker and Watts scheme is independent of cavity shape, it may be possible to reduce simulated solvent–solvent interactions to a very short range and correct using this reaction-field scheme. Conversely, the ion–solvent interactions would be calculated over as long a range as possible.

C. Generalized reaction field

The generalized reaction field (GRF) is another type of reaction-field correction to the truncated Coulomb potential proposed by Hummer *et al.*[11] For this scheme, the effective potential is

$$f_I(r)=f_S(r)=\frac{1}{r}-\frac{12}{5R}+\frac{4r^2}{R^3}-\frac{3r^3}{R^4}+\frac{2r^5}{5R^6}, \tag{64}$$

where a constant term has been added to Hummer's expression to ensure continuity of the potential. The polarization for this interaction function with $R=R_{IS}=R_{SS}=1.0$, 1.2, 1.4, and 5.0 nm is shown in Fig. 5. This correction does not agree with the Born polarization, underestimating it at larger distances, producing negative values of $p(r)$ near the cutoff radii. Surprisingly, Hummer obtained free energy results

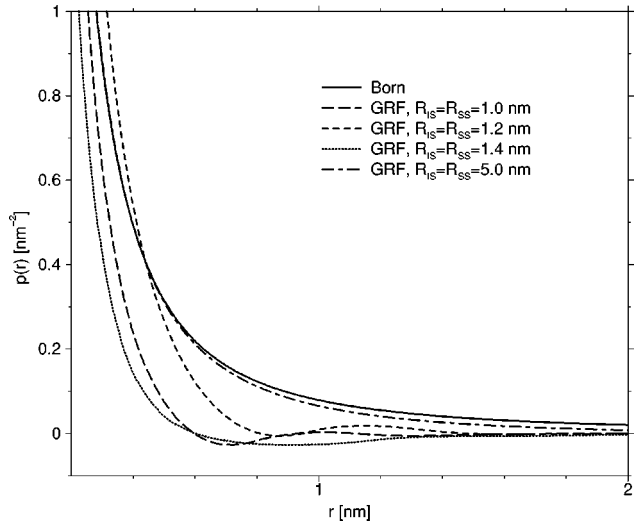

FIG. 5. Charge-scaled polarization for the GRF with interaction polynomials given by (64). $R_I=0.2$ nm, $\epsilon=78$, and $R_{IS}=R_{SS}=1.0$, 1.2, 1.4, and 5.0 nm. $p(r)$ is evaluated as for Figs. 2(a) and 2(b). The Born polarization is also displayed.

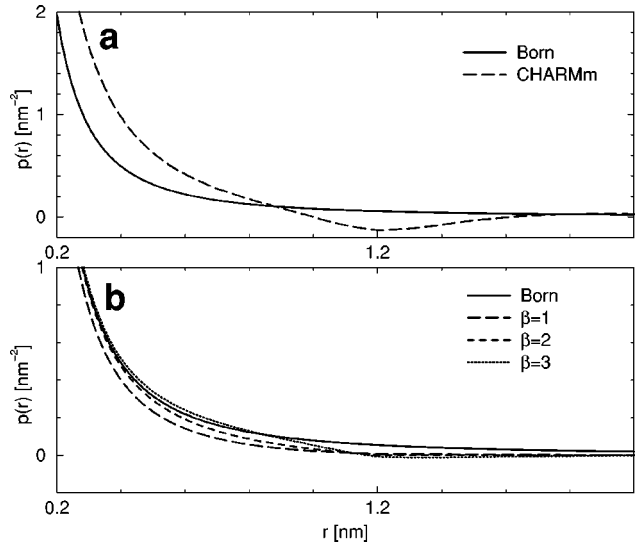

FIG. 6. Charge-scaled polarization for the shifting functions given by Eqs. (65) for (a) and (66) for (b) with orders $\beta=1,2,3$. $R_I=0.2$ nm, $\epsilon=78$, and $R_{IS}=R_{SS}=1.2$. nm $p(r)$ is evaluated as for Figs. 2(a) and 2(b). The Born polarization is also displayed.

with this correction method that agreed with the Born solvation free energy.[11] However, the GRF polarization functions obtained using the numerical methods of Appendix C (for $R=1.2$ nm, $R_I=0.2$ nm, and $\epsilon=78$) yields $\Delta G_{\text{solv}}=-242.452\,\text{kJ mol}^{-1}$. Even the inclusion of a ''self'' term $\Delta G_{\text{self}}=q^2\xi_{GRF}/(8\pi\epsilon_0)$, with $\xi_{GRF}\approx -12/(5R)$, to correct energy calculations[11] does not improve the performance, instead giving a corrected free energy of $-381.4\,\text{kJ mol}^{-1}$. This value does not agree with the Born solvation free energy of $-342.8\,\text{kJ mol}^{-1}$ as well as Hummer's reported results. However, as shown in Fig. 5, the agreement between the GRF and the Born polarization improves with increasing cutoff radius. Specifically, with a 5.0 nm cutoff distance, the uncorrected solvation free energy corresponding to the GRF model is $-290.03\,\text{kJ mol}^{-1}$, a value much closer to the Born solvation free energy than calculated for the smaller cutoff values.

Much of the discrepancy between the GRF and the Born model is found at distances close to the ion. In an actual simulation, the water molecules have a finite radius unlike the infinitesimal dipoles considered here. This finite radius could also contribute to the difference in the solvation free energies. The good results obtained by Hummer using the GRF model[46] may be due, in part, to this finite radius.

D. Shifting functions

Shifting functions provide another common correction to electrostatic truncation schemes. These functions tailor the electrostatic interactions to vanish smoothly at the cutoff distances. One common method, implemented in the CHARMm software, involves the ''shifted dielectric.''[53] Here the interaction functions have the form

$$f_I(r)=f_S(r)=\frac{1}{r}-\frac{2r}{R^2}+\frac{r^3}{R^4}. \tag{65}$$

Figure 6(a) depicts the charge-scaled polarization corresponding to this effective potential for $R=R_{IS}=R_{SS}=1.2$ nm. The polarization at short distances from the ion is dramatically overestimated, while its value near the cutoff radius is underestimated, even becoming negative.

An alternate scheme for shifting function correction is the generalized force shift, a method developed to allow an arbitrarily fast damping of the force near the cutoff radius.[34] The corresponding interaction polynomials have the form (corrected for a continuous potential at the cutoff distance)

$$f_I(r)=f_S(r)=\frac{1}{r}+\frac{r^\beta}{\beta R^{\beta+1}}-\frac{1}{R}+\frac{1}{\beta R}. \tag{66}$$

The charge-scaled polarization due to this method is shown in Fig. 6(b) for $\beta=1$, 2, and 3. Unlike the shifting function (65), this correction scheme causes the polarization to track more closely with the Born polarization below the cutoff radius. However, these functions still give solvation free energies that differ from the Born solvation energy by as much as $150\,\text{kJ mol}^{-1}$. The error from the implementation of shifting functions in simulation is well documented,[34,54–57] so the failure of these methods to give the Born result here is not surprising.

E. The optimal effective potential

Finally, the polarization corresponding to the optimum reaction field developed in Sec. II G is shown in Fig. 7. This figure depicts the approximate ($R_I=0$) analytic second-order correction as well as the second- and third-order corrections with coefficients obtained by numerical solution of Eqs. (53) and (54). Although the optimal effective potential tracks the Born polarization on both sides of the cutoff much more closely than other methods, it still consistently underestimates the polarization due to the ion. However, the amount by which the polarization is underestimated decreases with

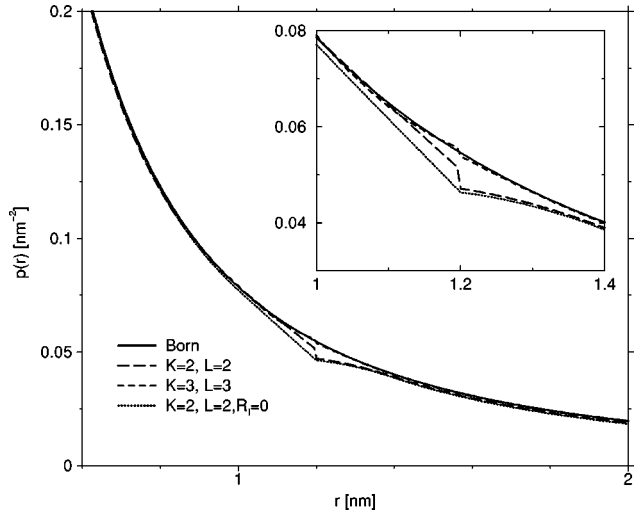

FIG. 7. Optimal effective potential, see Sec. II G. Evaluated with $\epsilon=78$ and $R_{IS}=R_{SS}=1.2$ nm. Analytical corrections (55) and (56) for $R_I=0$ nm are displayed with second- and third-order numerical optimal solutions for $R_I=0.2$ nm. The second-order optimal coefficients ($K=L=2$) are $a_{-1}=1.00$, $a_0=1.41\ \mathrm{nm}^{-1}$, $a_1=0.32\ \mathrm{nm}^{-2}$, $a_2=0.14\ \mathrm{nm}^{-3}$, $b_{-1}=1.00$, $b_0=0.60\ \mathrm{nm}^{-1}$, $b_1=-0.06\ \mathrm{nm}^{-2}$, and $b_2=-0.11\ \mathrm{nm}^{-3}$. Third-order optimal coefficients ($K=L=3$) are $a_{-1}=1.00$, $a_0=1.70\ \mathrm{nm}^{-1}$, $a_1=-0.03\ \mathrm{nm}^{-2}$, $a_2=1.30\ \mathrm{nm}^{-3}$, $a_3=-0.56\ \mathrm{nm}^{-4}$, $b_{-1}=1.00$, $b_0=-0.06\ \mathrm{nm}^{-1}$, $b_1=-0.58\ \mathrm{nm}^{-2}$, $b_2=-0.27\ \mathrm{nm}^{-3}$, $b_3-0.11\ \mathrm{nm}^{-4}$. $p(r)$ is evaluated as for Figs. 2(a) and 2(b). The Born polarization is also displayed for comparison.

increasing cutoff distances. The polarization due to this potential is continuous, but demonstrates a cusp at the truncation distance.

The fit of the optimal effective potential polarization to the Born polarization can be improved in several ways. In general, decreasing R_I or increasing R_{IS} and R_{SS} improves the agreement between the two potentials. Additionally, increasing the order (K and L) of the optimal interaction polynomials for the ion–solvent and solvent–solvent effective potentials also improves the agreement between the Born and optimal polarization. In general, this optimal potential agrees much more closely with the Born polarization than any other effective potentials examined in this work. However, none of the improvements completely removes the cusp in the polarization at the cutoff distance. Such discontinuities are often problematic for simulations, as they can lead to artificial ''heating'' of the solvent due to inaccurate forces.

IV. CONCLUSIONS

This report detailed the derivation and application of an integral equation for the polarization due to a single ion in a solvent continuum subject to electrostatic interaction schemes defined by arbitrary polynomials. The present study only considers the case of infinite dilution. However, this methodology can, in principle, be extended to include exponential terms which may arise from solutions to the Poisson–Boltzmann equation. The integral equation formalism was applied to several popular effective potentials used in molecular simulations. The results were compared with the Born polarization and solvation free energies to assess the performance of the different effective potentials. Finally, an optimal second-order effective potential was derived by variational treatment of the polarization integral equation under the simplifying assumptions of zero ionic radius. The optimal effective potential was found to provide the best agreement with the Born polarization among all the effective potentials considered in the present study.

The relevance of the observations of the present study can be evidenced by recalling four of the important issues facing simulations of ionic solvation involving electrostatic truncations

(I) Incorrect polarization of the solvent due to truncated (and possibly modified) interactions with surrounding solvent elements,

(II) Artifacts at the cutoff distance arising from the finite size of the solvent dipoles depending on the use of an atomic or charge-group cutoff,

(III) System-size dependent perturbation of the solvent due to artificial periodic boundary conditions,

(IV) Artificial heating during molecular dynamics simulation of molecules near the cutoff radius due to discontinuities in the forces.

This study details two possible methods for correcting the largest artifact (I) in explicit solvent ionic solvation simulations. First, the integral equation formalism can be used to derive corrections to the polarization and ionic solvation free energies for use after simulation with an arbitrary effective potential. Second, the optimal effective potential could be used in the simulation, in which case the results should be reasonably accurate in the absence of corrections. In general, the second choice is preferable in simulations where additional properties beyond the polarization and ionic solvation free energies are of interest.

The error arising from the neglect of finite dipole size (II) in treating the solvent near the cutoff radius has not been addressed in this study. Due to this finite size, simulated properties may vary considerably depending on whether the truncation is performed on an atomic or charge-group basis. For the case of pure water, it has been shown that charge-group truncation is the best choice for straight truncation of the Coulomb effective potential, while atom-based truncation is the best method when a Barker and Watts reaction-field correction is applied.[39] Several other groups[43–46] have investigated this phenomenon in ion solvation with straight Coulomb truncation and suggested corrections that could be easily implemented in conjunction with the methods outlined in this paper. In addition to such methods, an alternative scheme may eliminate the problem of finite dipole size. Using the charge-group truncation method as its basis, this scheme would progressively scale the interatomic distances and atomic charges of the solvent dipoles for distances between $R_{IS}-R_S$ and R_{IS}, where R_S is the radius of the solvent charge group. By scaling distances with a factor $\alpha=(R_{IS}-r_{CG})/R_S$ (for a solvent charge group separation of r_{CG}) and the charges by α^{-1}, the dipole moments of the solvent molecules would be preserved in the scaling. Such a dipole-switching scheme is currently under investigation.

Another type of artifact not discussed in this work involves the system-size dependence of simulated properties (III) due to the use of periodicity in many explicit solvent simulations.[7,11,39] In the specific case of truncated Coulomb

interactions, the perturbation of the solvation free energy of the ion in the central unit cell due to the presence of its periodic copies in the neighboring cells is quite small.[18] For other choices of effective potentials, the magnitude of the effect is likely to be correlated with the magnitude of the polarization outside the cutoff sphere of the ion. For all schemes discussed in present study, except the optimal effective potential, this polarization is small compared to the Born polarization implying the finite-size effects should be similarly small. A particularity interesting case is the Barker and Watts reaction-field correction (in the limit of infinite ϵ), where it was shown that the polarization is uniformly zero outside the cutoff sphere of the ion. Provided that the unit cell is larger than the cutoff sphere, this specific case should exhibit no finite-size effects arising from periodicity.

Finally, the artificial heating of molecules at distances close to the cutoff (IV) is caused by a nonvanishing radial component of the electrostatic field at the truncation radius. Again, the Barker and Watts reaction field (in the limit $\epsilon \rightarrow \infty$) overcomes this problem, by ensuring a vanishing force at the truncation radius.

In summary, the previous considerations lead to the following simulation scheme for the calculation of ionic solvation free energies using truncated electrostatic interactions. The Barker and Watts reaction-field (in the limit of infinite ϵ) should be used for both ion–solvent and solvent–solvent interactions to eliminate system-size effects arising from periodicity and to prevent heating due to cutoff noise. Using this effective potential, an analytical expression (44) is available for correcting the solvation free energy for inaccurate polarization of the solvent due to the effective potential. Finally, artifacts at the cutoff could be corrected by the dipole switching scheme suggested above, or by corrections analogous to those given in Refs. 18, 43, and 44. Explicit solvent simulations incorporating these principles are currently in progress to assess their ability to eliminate these four major sources of error and their compatibility with the results of simulations employing lattice sum methods.

The computation of accurate ionic solvation free energies by molecular simulations is appealing because, in contrast to the simple Born model derived from continuum electrostatics, they account for the detailed microscopic structure of the solvent molecules and the solvation shells. However, the solvation free energies obtained through these methods have proven to be extremely sensitive to the treatment of electrostatic interactions. Along with the present work, many recent advances[7,9,11,18] have contributed to elucidate some of the reasons for these discrepancies and have suggested the appropriate corrections. Owing to this significant progress, it is likely that in the very near future, molecular simulations will permit the calculation of methodology-independent ionic solvation free energies to be compared unambiguously with their experimental counterparts.

ACKNOWLEDGMENTS

This work was supported by grants from NSF, NIH, and SDSC. N.A.B. is a predoctoral fellow of the Howard Hughes Medical Institute. P.H.H. acknowledges support from the Human Frontier Science Program.

APPENDIX A: THE BORN LIMIT

To be valid, Eq. (32) must yield the Born polarization (36) as its solution in the limits $R_{IS}\rightarrow\infty$ and $R_{SS}\rightarrow\infty$ for a Coulomb potential ($a_k=0$ for all $k\neq -1$, $b_l=0$ for all $l\neq -1$). Since in this case, $g(r)=p_{\mathrm{Born}}(r)$, it is sufficient to prove that the integral term in (32) vanishes. The kernel is given by (25) and (35)

$$K(r,r') = \Psi_{-1}(r,r') = \frac{1}{8r^2R_{SS}^3}[(r^2-r'^2)^2-2R_{SS}^2(r^2+r'^2)+R_{SS}^4]. \tag{A1}$$

When $R_{SS}\rightarrow\infty$, $r'\gg r$ under the integral, and (A1) can be approximated as

$$K(r,r')\approx \frac{1}{8r^2R_{SS}^3}(r'^2-R_{SS}^2)^2. \tag{A2}$$

For large R_{SS} and for r' within the limits of integration, this function is always lower than its value at $w(r)$

$$\frac{1}{8r^2R_{SS}^3}[(r+R_{SS})^2-R_{SS}^2]^2=\frac{1}{8R_{SS}^3}(2R_{SS}+r)^2 \tag{A3}$$

and higher than its value at $v(r)$

$$\frac{1}{8r^2R_{SS}^3}[(r-R_{SS})^2-R_{SS}^2]^2=\frac{1}{8R_{SS}^3}(2R_{SS}-r)^2. \tag{A4}$$

Therefore, the integral is bounded by

$$\frac{r}{4R_{SS}^3}(2R_{SS}-r)^2p_{\min}\leqslant\int_{v(r)}^{w(r)}K(r,r')p(r')dr' \leqslant \frac{r}{4R_{SS}^3}(2R_{SS}+r)^2p_{\max}, \tag{A5}$$

where $p_{\max}$ and $p_{\min}$ are the maximum and minimum values of $p(r)$ on the interval $[v(r),w(r)]$. Assuming $p(r)$ is finite everywhere, $p_{\max}$ and $p_{\min}$ are finite, and both the upper and lower bounds in (A5) both vanish in the limit $R_{SS}\rightarrow\infty$ and the integral must therefore evaluate to zero. Consequently, (32) has the correct solution (36) in the case of a Coulomb potential.

APPENDIX B: NEUMANN SERIES SOLUTION OF INTEGRAL EQUATIONS

An analytical approach to the solution for $p(r)$ in (32) is given by a Neumann series. These series are approximate analytical solutions determined by successive substitutions of increasing accuracy and complexity. Such methods involve taking an initial guess for the solution and improving it iteratively by substitution into the integral equation.

The zero order approximation to $p(r)$ considers the first term of this series, namely, the inhomogeneous term of the integral equation,

$$p_0(r)=g(r), \tag{B1}$$

where the subscript denotes the order of the approximation. Substituting $p(r')$ by $p_0(r')$ in (32), gives the first-order approximation

$$p_1(r)=g(r)+\lambda\int_{v(r)}^{w(r)}K(r,r')g(r')dr'. \tag{B2}$$

The next iteration follows similarly

$$p_2(r)=g(r)+\lambda\int_{v(r)}^{w(r)}K(r,r')g(r')dr' + \lambda^2\int_{v(r)}^{w(r)}\int_{v(r')}^{w(r')}K(r,r')K(r',r'')g(r'')dr''dr'. \tag{B3}$$

This method can be viewed from a slightly different point of view by writing (32) in operator form

$$p(r)=g(r)+\lambda\hat{\mathcal{K}}p(r), \tag{B4}$$

where

$$\hat{\mathcal{K}}f(r)\equiv\int_{v(r)}^{w(r)}K(r,r')f(r')dr'. \tag{B5}$$

If the solution $p(r)$ exists, it may be written in terms of the inverse operation

$$p(r)=(1-\lambda\hat{\mathcal{K}})^{-1}g(r). \tag{B6}$$

A Neumann series approximates the solution by performing a Taylor series expansion of the inverse operator in (B6) around $\lambda=0$.[58,59] This yields the geometric series

$$(1-\lambda\hat{\mathcal{K}})^{-1}=\lim_{N\to\infty}\left[1+\sum_{n=1}^{N}\lambda^n\hat{\mathcal{K}}^n\right], \tag{B7}$$

for which convergence is not guaranteed.[58] Equations (B2) and (B3) represent the $N=0$, 1, or 2 approximations to (B7).

For the truncated Coulomb potential scheme (see Sec. III A) with $R_I=0$ and $R_{IS}=R_{SS}=R$, this method gives the zeroth-order approximation

$$p_0(r)=\frac{\lambda}{4\pi r^2}H(R-r) \tag{B8}$$

which is the truncated Born polarization (36). The first-order approximation is

$$p_1(r)=p_0(r)+\frac{\lambda^2}{6\pi R^3r^2}(r^3-R^3)H(R-r) + \frac{\lambda^2}{12\pi R^4r^2}\left(\frac{3r^4}{8}-Rr^3+2R^4\right)H(2R-r) \tag{B9}$$

and the second-order approximation is

$$p_2(r)=p_1(r)+\frac{\lambda^3}{4032\pi R^7r^2}(R-r)^4(-15r^3+17Rr^2 + 53R^2r+29R^3)H(R-r)\frac{\lambda^3}{10080\pi R^4r^2} \times(-105r^4+399R^2r^2-41R^4)H(2R-r). \tag{B10}$$

These functions are represented in Fig. 2(c) together with the numerical results based on the method of Appendix C. Finally, the second order approximation can be integrated over r as in (39) to obtain an analytic estimate for the solvation free energy corresponding to the truncated Coulomb scheme

$$\begin{aligned}\Delta G_{solv}&=-\frac{q_I^2}{2\epsilon_0}\int_{R_I}^{R}p_2(r')dr'\\ &=-\frac{q_I^2\lambda}{161280\pi\epsilon_0R^7R_I}\{[252(80+\lambda^2)R^6\\ &\quad+25(168+131\lambda)R^5R_I\lambda+(4200+503\lambda)\\ &\quad\times R^4R_I^2\lambda+3(280-229\lambda)R^3R_I^3\lambda\\ &\quad-267R^2R_I^4\lambda^2+258RR_I^5\lambda^2-50R_I^6\lambda^2]\\ &\quad\times(R-R_I)+1260R^6R_I\lambda^2\ln(R_I/R)\}.\end{aligned} \tag{B11}$$

APPENDIX C: NUMERICAL SOLUTION OF INTEGRAL EQUATIONS

The literature on numerical solutions of integral equations similar to Eq. (32) is substantial.[47,58,60–64] Such an integral equation can be recast into matrix equation form by projection onto a set of orthogonal functions or by discretization via a quadrature rule. Both of the methods discussed in this section involve discretization via a quadrature rule which turns the integral equation into a matrix inversion problem (Nystrom method,[58]). The interval of integration (R_I,R_{max}) is discretized into small distance elements Δr. For simplicity, Δr and R_{max} are chosen such that $R_I=N_I\Delta r$, $R_{SS}=N_{SS}\Delta r$, $R_{IS}=R_I+N_{IS}\Delta r$, and $R_{max}=R_I+(N_{max}-1)\Delta r$, where N_I, N_{SS}, N_{IS}, and N_{max} are all integers. The discretization occurs at the quadrature points $r_i=R_I+i\Delta r$ with $i\in(0,\ldots,N_{max-1})$ by the quadrature rule

$$p(r_i)=g(r_i)+\lambda\sum_{j=j_{min}}^{j_{max}}w_jK(r_i,r_j)p(r_j), \tag{C1}$$

where $\{w_j\}$ are the quadrature weights and

$$j_{min}=\max[0,i-N_{SS},N_{SS}-2N_I-i],$$

$$j_{max}=\min[i+N_{SS},N_{max}-1].$$

The simple trapezoidal quadrature rule is used here

$$w_j=\begin{cases}\Delta r/2 & \text{if } j=j_{min} \text{ or } j=j_{max}\\ \Delta r & \text{otherwise.}\end{cases} \tag{C2}$$

Upon discretization, the kernel can be represented as a $N_{max}\times N_{max}$ matrix K analogous to the operator $\hat{\mathcal{K}}$ defined in (B5), with elements

$$K_{ij}=\begin{cases}w_jK(R_I+i\Delta r,R_I+j\Delta r) & \text{if } j\geqslant j_{min} \text{ or } j\leqslant j_{max}\\ 0 & \text{otherwise.}\end{cases} \tag{C3}$$

Denoting the solution at the quadrature points r_i as the N_{max}-dimensional vector $\mathbf{p}$ and defining an analogous vector $\mathbf{g}$ for the inhomogeneous term, (C1) becomes

$$\mathbf{p}=(\mathsf{I}-\lambda\mathsf{K})^{-1}\mathbf{g}, \tag{C4}$$

where I is the $N_{\max}\times N_{\max}$ identity matrix. The inverse matrix $(\mathsf{1}-\lambda\mathsf{K})^{-1}$ in (C4) is analogous to the operator $(1-\lambda\hat{\mathcal{K}})^{-1}$ in (B6). The solution of the integral equation is thus turned into a simple matrix inversion problem.[58] Various methods for performing such inversions are given in Ref. 64. In the present work, LU decomposition of the matrix equation with backsubstitution was used.[51]

The solvation free energy (39) can also be calculated from $p(r)$ via a quadrature method. Specifically, this work uses a discretization scheme similar to that used by Wood[18]

$$
\begin{aligned}
k\int_{R_{\mathrm{I}}}^{R_{\mathrm{IS}}} p(r')r'^{k+1}dr' &\approx \sum_{i=1}^{N_{\mathrm{IS}}-1} r_i^2\left[\left(r_i+\frac{\Delta r}{2}\right)^k-\left(r_i-\frac{\Delta r}{2}\right)^k\right]p(r_i)\\
&\quad+R_{\mathrm{I}}^2\left[\left(R_{\mathrm{I}}+\frac{\Delta r}{2}\right)^k-R_{\mathrm{I}}^k\right]p(R_{\mathrm{I}})+R_{\mathrm{IS}}^2\\
&\quad\times\left[R_{\mathrm{IS}}^k-\left(R_{\mathrm{IS}}-\frac{\Delta r}{2}\right)^k\right]p(R_{\mathrm{IS}}). \qquad \text{(C5)}
\end{aligned}
$$

[1] S. C. Harvey, Proteins: Struct., Funct., Genet. **5**, 78 (1989).
[2] M. E. Davis and J. A. McCammon, Chem. Rev. **90**, 509 (1990).
[3] H. J. C. Berendsen, in *Computer Simulation of Biomolecular Systems, Theoretical and Experimental Applications*, edited by W. F. van Gunsteren, P. K. Weiner, and A. J. Wilkinson (ESCOM, Leiden, The Netherlands, 1993), Vol. II, pp. 161–181.
[4] P. Smith and W. F. van Gunsteren, in *Computer Simulation of Biomolecular Systems, Theoretical and Experimental Applications*, edited by W. F. van Gunsteren, P. K. Weiner, and A. J. Wilkinson (ESCOM, Leiden, The Netherlands, 1993), Vol. II, pp. 182–212.
[5] R. M. Levy and E. Gallicchio, Annu. Rev. Phys. Chem. **49**, 531 (1998).
[6] B. Luty, I. Tironi, and W. van Gunsteren, J. Chem. Phys. **103**, 3014 (1995).
[7] F. Figueirido, G. S. Del Buono, and R. M. Levy, J. Phys. Chem. B **101**, 5622 (1997).
[8] B. A. Luty and W. F. van Gunsteren, J. Chem. Phys. **100**, 2581 (1996).
[9] P. H. Hünenberger and J. A. McCammon, J. Chem. Phys. **110**, 1856 (1999).
[10] P. H. Hünenberger and J. A. McCammon, Biophys. Chem. (in press).
[11] G. Hummer, L. R. Pratt, and A. E. García, J. Phys. Chem. **100**, 1206 (1996).
[12] G. Hummer, L. R. Pratt, and A. E. García, J. Chem. Phys. **107**, 9275 (1997).
[13] G. Hummer, L. R. Pratt, and A. E. García, J. Phys. Chem. A **102**, 7885 (1998).
[14] M. Neumann, Mol. Phys. **50**, 841 (1983).
[15] M. Neumann, O. Steinhauser, and G. S. Pawley, Mol. Phys. **52**, 97 (1984).
[16] C. L. Brooks III, B. M. Pettitt, and M. Karplus, J. Chem. Phys. **83**, 5897 (1985).
[17] P. Linse and H. C. Andersen, J. Chem. Phys. **85**, 3027 (1986).
[18] R. H. Wood, J. Chem. Phys. **103**, 6177 (1995).
[19] C. L. Brooks III, J. Chem. Phys. **86**, 5156 (1987).
[20] J. F. Madura and B. M. Pettitt, Chem. Phys. Lett. **150**, 105 (1988).
[21] T. P. Straatsma and H. J. C. Berendsen, J. Chem. Phys. **89**, 5876 (1989).
[22] S. Sakane, H. S. Ashbaugh, and R. H. Wood, J. Phys. Chem. B **102**, 5673 (1998).
[23] B. M. Pettitt and P. J. Rossky, J. Chem. Phys. **84**, 5836 (1986).
[24] L. X. Dang and B. M. Pettitt, J. Phys. Chem. **94**, 4303 (1990).
[25] E. Guàrdia, R. Rey, and J. A. Padró, J. Chem. Phys. **95**, 2823 (1991).
[26] L. X. Dang, B. M. Pettitt, and P. M. Rossky, J. Chem. Phys. **96**, 4046 (1992).
[27] J. S. Bader and D. Chandler, J. Phys. Chem. **96**, 6423 (1992).
[28] G. Hummer, D. M. Soumpasis, and M. Neumann, Mol. Phys. **81**, 1155 (1993).
[29] P. E. Smith and B. M. Pettitt, J. Chem. Phys. **95**, 8430 (1991).
[30] H. Schreiber and O. Steinhauser, Biochemistry **31**, 5856 (1992).
[31] H. Schreiber and O. Steinhauser, Chem. Phys. **168**, 75 (1992).
[32] H. Schreiber and O. Steinhauser, J. Mol. Biol. **228**, 909 (1992).
[33] R. J. Loncharich and B. R. Brooks, Proteins: Struct., Funct., Genet. **6**, 32 (1989).
[34] P. J. Steinbach and B. R. Brooks, J. Comput. Chem. **15**, 667 (1994).
[35] J. Barker and R. Watts, Mol. Phys. **26**, 789 (1973).
[36] H. Alper and R. M. Levy, J. Chem. Phys. **91**, 1242 (1989).
[37] G. Hummer and D. M. Soumpasis, J. Phys.: Condens. Matter **6**, A141 (1994).
[38] I. G. Tironi, R. Sperb, P. E. Smith, and W. F. van Gunsteren, J. Chem. Phys. **102**, 5451 (1995).
[39] P. H. Hünenberger and W. F. van Gunsteren, J. Chem. Phys. **108**, 6117 (1998).
[40] H. Resat and J. A. McCammon, J. Chem. Phys. **104**, 7645 (1996).
[41] M. Born, Z. Phys. **1**, 45 (1920).
[42] B. Roux, Y. Hsiang-Ai, and M. Karplus, J. Phys. Chem. **94**, 4683 (1990).
[43] G. Hummer, L. R. Pratt, A. E. García, B. J. Berne, and S. W. Rick, J. Phys. Chem. B **101**, 3017 (1997).
[44] H. S. Ashbaugh and R. H. Wood, J. Chem. Phys. **106**, 8135 (1997).
[45] J. Åqvist and T. Hansson, J. Phys. Chem. B **102**, 3837 (1998).
[46] G. Hummer, L. R. Pratt, A. E. García, S. Garde, B. J. Berne, and S. W. Rick, J. Phys. Chem. B **102**, 3841 (1998).
[47] G. B. Arfken and H. J. Weber, *Mathematical Methods for Physicists*, 4th ed. (Academic Press, San Diego, CA, 1995).
[48] J. Jackson, *Classical Electrodynamics*, 2nd ed. (Wiley, New York, 1975).
[49] P. M. Morse and H. Feshbach, *Methods of Theoretical Physics, Part I* (McGraw–Hill, New York, 1953).
[50] J. Mathews and R. Walker, *Mathematical Methods of Physics*, 2nd ed. (Addison–Wesley, Redwood City, CA, 1970).
[51] P. H. Hünenberger, A C program to solve integral equations as described in Appendix B.
[52] S. Wolfram, *The Mathematica Book*, 3rd ed. (Wolfram Media, Champaign, IL, 1996).
[53] B. R. Brooks, R. E. Bruccoleri, B. A. Olafson, D. J. States, A. Swaminathan, and M. Karplus, J. Comput. Chem. **4**, 187 (1983).
[54] G. S. Del Buono, F. E. Figueirido, and R. M. Levy, Chem. Phys. Lett. **263**, 521 (1996).
[55] G. S. Del Buono, T. S. Cohen, and P. J. Rossky, J. Mol. Liq. **60**, 221 (1994).
[56] K. F. Lau, H. E. Alper, T. S. Thatcher, and T. E. Stouch, J. Phys. Chem. **98**, 8785 (1994).
[57] L. Perera, U. Essmann, and M. L. Berkowitz, J. Chem. Phys. **102**, 450 (1994).
[58] L. Delves and J. Mohamed, *Computational Methods for Integral Equations* (Cambridge University Press, New York, 1985).
[59] J. Irving and N. Mullineux, *Mathematics in Physics and Engineering* (Academic, New York, 1959).
[60] M. Golberg and C. Chen, *Discrete Projection Methods for Integral Equations* (Computational Mechanics Publications, Boston, MA, 1997).
[61] K. E. Atkinson, *A Survey of Numerical Methods for the Solution of Fredholm Integral Equations of the Second Kind* (SIAM, Philadelphia, 1976).
[62] L. Delves and J. Walsh, *Numerical Solution of Integral Equations* (Oxford University Press, New York, 1974).
[63] C. Green, *Integral Equation Methods* (Nelson, London, 1969).
[64] W. H. Press, W. T. Teukolsky, and B. P. Flannery, *Numerical Recipes in C: The Art of Scientific Computing*, 2nd ed. (Cambridge Press, New York, 1992).